POLITECNICO DI TORINO
Repository ISTITUZIONALE

On the use of the inverse finite element method to enhance knowledge sharing in population-based structural health monitoring

Original
On the use of the inverse finite element method to enhance knowledge sharing in population-based structural health monitoring / Delo, Giulia; Roy, Rinto; Worden, Keith; Surace, Cecilia. - In: COMPUTERS & STRUCTURES. - ISSN 0045-7949. - 307:(2025). [10.1016/j.compstruc.2024.107635]

Availability:
This version is available at: 11583/2995988 since: 2024-12-28T07:29:47Z

Publisher:
Elsevier

Published
DOI:10.1016/j.compstruc.2024.107635

Terms of use:

This article is made available under terms and conditions as specified in the corresponding bibliographic description in the repository

Publisher copyright

(Article begins on next page)

27 April 2026

Computers and Structures 307 (2025) 107635

Contents lists available at ScienceDirect

Computers and Structures

journal homepage: www.elsevier.com/locate/compstruc

On the use of the inverse finite element method to enhance knowledge sharing in population-based structural health monitoring

Giulia Delo [a,*], Rinto Roy [b], Keith Worden [c], Cecilia Surace [b]

[a] Department of Mechanical and Aerospace Engineering, Politecnico di Torino, Corso Duca degli Abruzzi, 24, Torino, 10129, Italy
[b] Department of Structural, Geotechnical and Building Engineering, Politecnico di Torino, Corso Duca degli Abruzzi, 24, Torino, 10129, Italy
[c] Dynamics Research Group, Department of Mechanical Engineering, University of Sheffield, Mappin Street, Sheffield, S1 3JD, UK

ARTICLE INFO

Keywords:
Inverse finite element method (iFEM)
Population-based structural health monitoring (PBSHM)
Damage diagnosis
Deformation reconstruction
Frequency response functions (FRFs)
Transfer component analysis (TCA)

ABSTRACT

Efficient Structural Health Monitoring (SHM) is critical for ensuring safety and improving the operation and maintenance of aerospace structures. This study focusses on advanced shape-sensing methods, such as the inverse Finite Element Method (iFEM), which can estimate the complete displacement field of a structure based on a restricted number of strain measurements, fostering continuous and real-time monitoring. This approach additionally provides valuable insights into the dynamic behaviour of a structure by extracting its Frequency Response Functions (FRFs) and modal properties to perform vibration-based SHM. However, effectively extending SHM to a fleet or population of structures would require a significant amount of data for each one, which may be unavailable or incomplete. A population-based Structural Health Monitoring (PBSHM) strategy can solve data scarcity by sharing knowledge between similar structures via transfer-learning algorithms. In PBSHM, handling data from diverse sources is paramount for achieving accurate results. Therefore, this study integrates iFEM into the PBSHM framework, enhancing knowledge transfer by harmonising fibre-optic strain measurements to vibration-based features and providing reliable source data to inform diagnostics on similar structures. The proposed approach is validated on a population of laboratory-scale steel aircraft subjected to specific operating and damage conditions tested using three different sensor setups.

1. Introduction

The ageing of structures, along with the challenges related to fatigue loadings and the ongoing growth in the aerospace industry, led to the development of advanced techniques, experimental methods, and refined data-processing algorithms for monitoring aircraft structural integrity, pushing the boundaries of durability and ensuring sustained operational quality. As aircraft endure prolonged service periods and face diverse and challenging conditions during flight, assessing their mechanical behaviour and identifying potential damage becomes of paramount concern. These needs gave rise to the Structural Health Monitoring (SHM) field in aerospace engineering for early damage detection, real-time assessment of structural components and effective maintenance management. The SHM evolution has been significantly advanced by recent progress in sensor technologies and data processing capabilities, which have facilitated more efficient monitoring systems compared to the commonly adopted non-destructive tests (NDTs). Indeed, NDTs based on on-ground visual or ultrasonic inspections are expensive and often ineffective. However, the application of SHM techniques in the aerospace field may be limited by the complexity of geometries, the large amount of sensors and data required, and the feasibility of these approaches under different damage scenarios, and changing environmental and operational conditions [1].

In this framework, significant efforts concern shape-sensing approaches, which allow reconstruction of structural displacements from a limited number of measurements [2,3], reducing the required economic and human resources and leading to a condition-based maintenance strategy [4]. These approaches exploit distributed fibre-optic sensors [5], strain gauges, and computer-vision techniques [6], enhancing real-time monitoring of structural deformation. Shape sensing offers various applications in SHM, including anomaly detection and delamination identification in composite materials [7]. In addition, algorithms such as Smoothing Element Analysis (SEA) [8] and inverse Finite Element Method (iFEM) allow for studying optimal sensor placement and shape-morphing structures.

* Corresponding Author.
E-mail address: giulia.delo@polito.it (G. Delo).

https://doi.org/10.1016/j.compstruc.2024.107635
Received 6 June 2024; Accepted 18 December 2024

0045-7949/© 2024 The Author(s). Published by Elsevier Ltd. This is an open access article under the CC BY license (http://creativecommons.org/licenses/by/4.0/).

Among the possible shape-sensing strategies, the current study focuses on iFEM, which has been proposed by Tessler and Spangler [9,10] for plates and shell structures. This method involves a least-squares minimisation of a functional that represents a weighted difference between the experimentally-measured strains and those coming from a finite-element approximation. The discretisation of the structure is similar to the one proposed in the Finite Element Method (FEM). However, this shape-sensing approach does not need information regarding the material and the damping properties, or the external loadings applied on the structure [9]. The iFEM shape-sensing formulation has been extended for a variety of systems, including trusses, beams, and frames [11–13], thin-walled structures [14,15], and complex statically-loaded structures [16]. Recent studies implemented IFEM to perform SHM of an offshore wind turbine [17], monitoring its stresses and displacements under multiple loading conditions. Li et al. [18] proposed a damage-identification approach based on iFEM strain data and convolutional neural networks to locate and quantify numerically simulated damage. In addition, iFEM has been proposed to automate crack size assessment by introducing damage modelling within the iFEM framework and selecting the most accurate damage scenario with respect to the experimental measurements [19]. Moreover, iFEM has been combined with Modal Virtual Sensor Expansion in [20] to enhance the shape-sensing accuracy of composite stiffened structures using a reduced number of strain sensors. Furthermore, recent developments proposed an extension of the iFEM methodology to also investigate dynamic responses. Indeed, [21] shows experimentally how the displacements reconstructed from dynamic strain measurements using iFEM can provide valuable insights into the dynamic behaviour of a structure, enabling the extraction of its Frequency Response Functions (FRFs) and modal properties. A similar workflow has been presented in [22], in which the dynamic response of a numerically simulated plate under undamaged and damaged conditions is reconstructed by examining the iFEM response within the frequency domain.

The capability of reconstructing the classical Experimental Modal Analysis (EMA) features enables iFEM to be exploited in the field of vibration-based SHM, which includes different non-intrusive and damage-sensitive methodologies for assessing the behaviour of existing structures. The vibration-based approaches to SHM are commonly distinguished as model-based and data-driven ones. Specifically, data-driven SHM includes a set of robust and effective algorithms, inspired by the fields of machine learning and pattern recognition [23,24]. These algorithms are trained on sufficiently large datasets, to build SHM models according to the level of diagnosis required, i.e., identification models for damage detection, classification models for damage localisation, or regression models for quantification tasks [25]. However, their feasibility is often limited because of the lack of complete or sufficient data. Collecting labelled training data for each structure, considering various operational conditions and damage states, would be expensive and frequently unrealistic [26]. In this framework, recent studies are developing a population-based Structural Health Monitoring (PBSHM) theory, intended to address the data-scarcity challenge, by sharing knowledge across a population of similar structures.

The PBSHM theory, described in [27–30], proposes adopting some classes of transfer-learning algorithms, e.g., domain adaptation [26], to share information gathered from a source structure for improving diagnostic inferences on a new target structure. This approach comprises several phases, including identifying the degree of similarity between two structures [31,32], and their datasets, selecting the most suitable features for transfer, and investigating the most effective algorithms for this purpose. Therefore, it is necessary to distinguish between homogeneous and heterogeneous populations. Homogeneous populations comprise only nominally-identical systems [28]. For instance, these populations could include a fleet composed of analogous aircraft, in which the only differences regard manufacturing variations. Instead, heterogeneous populations can include more diverse systems, presenting variations in their geometry, dimensions, materials or topological properties [29]. Heterogeneous populations distinctly require a phase of similarity assessment to limit the risk of negative transfer [33], the phenomenon occurring when the knowledge shared from a source structure lowers the diagnostic performance on the target structure. Different approaches have been proposed for assessing similarity in heterogeneous populations and to determine the value of knowledge transfer [34,35], and a novel possibility in this field adopts the available mode shapes to measure the similarity between source and target structures employing the modal assurance criterion, as shown in [36]. Afterwards, if the systems are defined sufficiently similar, their features can be involved in knowledge sharing.

Nevertheless, when sharing data in real-life scenarios, it is necessary to consider the varying experimental setups, sensors, inputs, and acquisition systems that may affect the resulting features. This feature variability may induce a robustness and feasibility reduction in the PBSHM approach. Thus, the work presented in [21] proposed an iFEM-based approach to reconstruct the modal parameters and presented detailed results of the experimental validation campaign. The experimental results showed the added value of iFEM compared to more classical techniques, particularly in its ability to capture the global dynamic response and modal parameters of the analysed structure from a cost-effective sensor scheme, aligning strain-based results with the traditional damage-sensitive features used in vibration-based SHM. In contrast, more classical techniques require a significant amount of sensors, or can only capture the FRF at a single location, which is insufficient for analysing the structure's overall dynamic behaviour, limiting the approach to a more localised perspective. Indeed, in these cases, an a priori knowledge of the critical location would be required. In contrast, the iFEM approach enables the reconstruction of displacements, FRFs and mode shapes globally across the structure. The current work extends this study by proving how iFEM can enhance knowledge transfer by harmonising results acquired from different tests and effectively managing heterogeneous data types. Therefore, via iFEM dynamic displacement reconstruction, it is possible to provide real-time reliable source features which can inform diagnostics on similar structures, facilitating PBSHM applicability even under varying experimental approaches.

The shape-sensing methodology is integrated into the PBSHM framework as a preliminary feature-harmonisation tool, to reconstruct the dynamic full-field displacements of a source structure and extract damage-sensitive features, adopting the procedure described in [21]. These features are adopted as training data in a domain-adaptation algorithm, i.e., the Transfer Component Analysis (TCA) [37,38]. The TCA learns a transformation to map the source and target features into a common latent space, where damage detection can be performed based on data from both domains, by measuring the Mahalanobis-Squared-Distance (MSD) between the features. This approach is validated here in two experimental case studies involving similar laboratory-scale steel aircraft subjected to specific operating and damage conditions tested using three different sensors, i.e., high-definition distributed fibre-optic strain sensors, Scanning Laser Doppler Vibrometer (SLDV) and Integrated Circuit Piezoelectric accelerometers. The first case study regards almost identical structures and different sensors. Thus, it is possible to prove how iFEM can solve the issues regarding different sensors by harmonising the features in a homogeneous population. The second case study assesses more dissimilar structures to illustrate how iFEM can facilitate PBSHM by producing reliable source knowledge in a heterogeneous population.

The layout of the paper is as follows. Section 2 presents the adopted methodologies, including the iFEM formulation, its implementation in a dynamic framework for FRF reconstruction, and the class of domain-adaptation algorithms, focussing on Transfer Component Analysis. Section 3 illustrates the experimental case study regarding a population of aircraft tested under undamaged and damaged conditions. Section 4 presents the results of the proposed damage detection and classification approach. Subsequently, some discussions and conclusions are provided in Section 5.

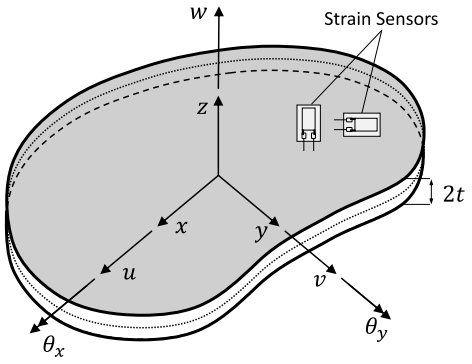

Fig. 1. Plate geometry, kinematic variables, and instrumented sensors.

2. Methods

2.1. Dynamic shape-sensing using iFEM and FRF reconstruction

The current section describes the iFEM shape-sensing formulation and its implementation for reconstructing dynamic features, such as FRFs and modal parameters. Consider a plate domain, Ω, defined in the three-dimensional Cartesian coordinate frame, $\Omega = (x, y, z) \subset R^3$, of thickness $2t$ and mid-plane positioned at $z = 0$ ($(x, y) \in A \subset R^2$), where A is the mid-plane area. The plate is subjected to external in-plane or out-of-plane loads and information of the resulting strain field is obtained using sensors placed at N discrete in-plane locations $(x, y)_i$, $i = 1, .., N$. Each site has strain sensors instrumented on both the top and bottom surfaces measuring strain components $\boldsymbol{\varepsilon}_i^+ = \{\varepsilon_{xx}^+, \varepsilon_{yy}^+, \gamma_{xy}^+\}_i^T$ and $\boldsymbol{\varepsilon}_i^- = \{\varepsilon_{xx}^-, \varepsilon_{yy}^-, \gamma_{xy}^-\}_i^T$, respectively. Reconstruction of the three-dimensional plate deformations based on the discrete strain measurements, given no load or material information, is an inverse problem of relevance for the present work. iFEM is used to provide a variationally-based solution to this problem and its underlying theory is briefly presented in this section. Interested readers can refer Tessler and Spangler [10] for more details of the iFEM formulation.

Based on the kinematic assumptions of Mindlin plate theory, the Cartesian components of the displacement vector of any material point are given as,

$$\begin{aligned} u_x(x, y, z) &= u(x, y) + z\theta_y(x, y), \\ u_y(x, y, z) &= v(x, y) - z\theta_x(x, y), \\ u_z(x, y, z) &= w(x, y), \end{aligned} \tag{1}$$

where the kinematic variables u and v are the mid-plane displacements in the x and y directions, respectively; w is average transverse deflection; and θ_x and θ_y are the section rotations about the x and y axes, respectively (see Fig. 1).

The linear strain-displacement relations give rise to the following in-plane, bending, and transverse shear-strain relations in terms of the kinematic variables,

$$\begin{aligned} \begin{Bmatrix} \varepsilon_{xx} \\ \varepsilon_{yy} \\ \gamma_{xy} \end{Bmatrix} &= \begin{Bmatrix} u_{,x} \\ v_{,y} \\ u_{,y} + v_{,x} \end{Bmatrix} + z \begin{Bmatrix} \theta_{y,x} \\ -\theta_{x,y} \\ -\theta_{x,x} + \theta_{y,y} \end{Bmatrix} = \mathbf{e}(\mathbf{u}) + z\mathbf{k}(\mathbf{u}), \\ \begin{Bmatrix} \gamma_{xz} \\ \gamma_{yz} \end{Bmatrix} &= \begin{Bmatrix} w_{,x} + \theta_y \\ w_{,y} - \theta_x \end{Bmatrix} = \mathbf{g}(\mathbf{u}), \end{aligned} \tag{2}$$

where $\mathbf{u} \equiv \{u, v, w, \theta_x, \theta_y\}^T$ is a vector of kinematic variables and $\mathbf{e}$, $\mathbf{k}$, and $\mathbf{g}$ are strain measures representing the in-plane stretching, curvature, and transverse shear of the mid-plane, respectively.

At discrete plate locations $(x, y)_i$ where sensors are used to measure strains on the top and bottom surfaces, the measured strains can be related to the mid-plane strain measures via the following relations,

$$\mathbf{e}_i^\varepsilon = \frac{1}{2}\left(\begin{Bmatrix} \varepsilon_{xx}^+ \\ \varepsilon_{yy}^+ \\ \gamma_{xy}^+ \end{Bmatrix} + \begin{Bmatrix} \varepsilon_{xx}^- \\ \varepsilon_{yy}^- \\ \gamma_{xy}^- \end{Bmatrix}\right)_i, \quad \mathbf{k}_i^\varepsilon = \frac{1}{2t}\left(\begin{Bmatrix} \varepsilon_{xx}^+ \\ \varepsilon_{yy}^+ \\ \gamma_{xy}^+ \end{Bmatrix} - \begin{Bmatrix} \varepsilon_{xx}^- \\ \varepsilon_{yy}^- \\ \gamma_{xy}^- \end{Bmatrix}\right)_i, \quad i = 1, .., N, \tag{3}$$

where the ε superscript denotes the experimental nature of these quantities.

The iFEM methodology is based on minimising, in a least-squares sense, the difference between the analytical and experimental strain measures defined in Eq. (2) and (3), respectively; it can be implemented in a piece-wise continuous manner based on the finite-element framework. The plate domain is discretised using two-dimensional inverse finite elements, and for each element, e, a weighted least-squares error functional is formulated as,

$$\Phi^e(\mathbf{u}^e) \equiv \mathbf{w}_e||\mathbf{e}(\mathbf{u}^e) - \mathbf{e}^\varepsilon||^2 + \mathbf{w}_k||\mathbf{k}(\mathbf{u}^e) - \mathbf{k}^\varepsilon||^2 + \mathbf{w}_g||\mathbf{g}(\mathbf{u}^e) - \mathbf{g}^\varepsilon||^2, \tag{4}$$

where $\mathbf{w}_e$, $\mathbf{w}_k$, and $\mathbf{w}_g$, are vectors of weighting coefficients that control the degree of enforcement between the analytical and experimental strain measures. The individual error norms (for an element with area A_e) are given as,

$$\begin{aligned} ||\mathbf{e}(\mathbf{u}^e) - \mathbf{e}^\varepsilon||^2 &= \frac{1}{A_e}\int_{A_e} [\mathbf{e}(\mathbf{u}^e) - \mathbf{e}^\varepsilon]^2 dA, \\ ||\mathbf{k}(\mathbf{u}^e) - \mathbf{k}^\varepsilon||^2 &= \frac{(2t)^2}{A_e}\int_{A_e} [\mathbf{k}(\mathbf{u}^e) - \mathbf{k}^\varepsilon]^2 dA, \\ ||\mathbf{g}(\mathbf{u}^e) - \mathbf{g}^\varepsilon||^2 &= \frac{1}{A_e}\int_{A_e} [\mathbf{g}(\mathbf{u}^e)]^2 dA. \end{aligned} \tag{5}$$

When experimental strain measurements are available for an inverse element, the corresponding weighting coefficients are set to unity. Otherwise, they are set to a small value (10^{-5}) to reduce the element contribution in the global functional. As $\mathbf{g}^\varepsilon$ cannot be computed directly from experimental measurements, the squared-norm form of Eq. (5) is used and $\mathbf{w}_g$ is set to a small value.

The element error functional of Eq. (4) is minimised with respect to the nodal degrees-of-freedom to obtain the element-level equation: $\mathbf{k}^e\mathbf{u}^e = \mathbf{f}^e$. Appropriate coordinate transformations are applied and the element contributions are assembled into a global system of equations. Problem-specific displacement boundary conditions are enforced to obtain the final global matrix equation:

$$\mathbf{KU} = \mathbf{F}. \tag{6}$$

The unknown nodal displacements can be computed using $\mathbf{U} = \mathbf{K}^{-1}\mathbf{F}$. As $\mathbf{K}$ is only a function of the sensor positions, it is only inverted once for a specific sensor layout. The vector $\mathbf{F}$ is dependent on both sensor positions and measurements and is recomputed for each new strain acquisition step. Once $\mathbf{F}$ is updated at each time step, the displacement field can be computed with minimal computational effort, making iFEM appealing for dynamic applications as discussed in the present work. Indeed, the reconstructed displacement time history and the input signal (acquired using a load cell), can be processed via the Fast Fourier Transform (FFT) to compute the response and the input in the frequency domain. Afterwards, the output and input measurements are used to estimate the FRFs and identify the modal parameters. For further details of the reconstruction and identification of modal parameters using iFEM, readers can refer to [21]. This methodology facilitates the employment of iFEM-reconstructed parameters for vibration-based SHM and global damage detection. Indeed, vibration-based SHM often investigates the global behaviour of a structure by identifying its dynamic properties and extracting effective features sufficiently sensitive to the possible damage scenarios, which are analysed to monitor the overall health of the structure [39]. In contrast, when the vicinity of the damage location is known a priori, strain-based approaches may be used for local damage

identification. In this framework, iFEM can detect local changes induced by damage, but it can also provide a global analysis of a structure as it reconstructs its full-field displacements. Moreover, the proposed method gathers the global damage-sensitive features usually adopted in vibration-based SHM from cost-effective fibre-optic sensors. Thus, the current approach enhances traditional vibration-based SHM and PBSHM by efficiently providing global features to study the overall behaviour of a structure and transfer this knowledge to similar ones, while additionally providing the local insights of strain-based approaches.

2.2. Domain adaptation via transfer component analysis

The advent of machine learning and pattern recognition methods has facilitated the development of a range of data-based techniques within the SHM field. These techniques leverage dynamic features such as modal properties and transfer functions to enable efficient diagnostic performance, especially for analysing large volumes of data and identifying patterns that are not easily discernible by traditional SHM methods [24,39]. However, sufficient training data are not often available. In addition, the training and test data should come from the same domain, and have the same distribution [37]. In these scenarios, transfer-learning algorithms can improve diagnostic inferences by sharing knowledge from a more comprehensive source domain to a potentially different target domain.

Different transfer-learning algorithms can be employed based on the type of features, monitoring task, and available data [40]. The current study considers features extracted from dynamic transfer functions. It assumes that the target domain does not include any samples from damaged conditions in the training dataset, but only a limited number of samples from a healthy condition. Therefore, it is necessary to inform a damage-detection model using additional samples from a source domain, which includes a more extensive and complete training dataset. The algorithm that has been implemented for the purpose of this SHM task is the TCA. This transfer learning strategy is part of the class of domain adaptation, and it learns a nonlinear mapping between the features of the source and target structures and transforms them into a low-dimensional latent space by minimising the difference between their marginal probability distributions [37,41].

In order to describe the TCA algorithm, it is necessary to define the concepts of domain, task and the main principles of transfer learning. A domain $\mathcal{D}$ is composed of a feature space χ, and a marginal probability distribution $P(X)$, where $X = \{x_1, x_2, ...x_n\} \in \chi$. A task $\mathcal{T}$ is composed of a label space $\mathcal{Y}$, where $Y = \{y_1, y_2, ...y_n\} \in \mathcal{Y}$, and a predictive function $P(y_i|x_i)$, which should be estimated from the data during the training phases. In this study, the features are segments of an averaged FRF, while the labels are indicators of damage. A transfer-learning algorithm is a particular machine-learning strategy which tries to accurately build a predictive function on a target domain $\mathcal{D}_T$, exploiting the source domain $\mathcal{D}_S$ and task $\mathcal{T}_S$, assuming that $\mathcal{D}_T \neq \mathcal{D}_S$ or $\mathcal{T}_T \neq \mathcal{T}_S$. Domain adaptation is a class of transfer learning which assumes that $\mathcal{D}_T \neq \mathcal{D}_S$, but $P(Y_S|X_S) = P(Y_T|X_T)$.

TCA is a domain-adaptation approach which performs harmonisation and dimensionality-reduction of the original features. This algorithm learns a transformation ψ such that $P(\psi(X_S)) \approx P(\psi(X_T))$, and also assumes $P(Y_S|\psi(X_S)) \approx P(Y_T|\psi(X_T))$. The distance between the marginal probability distributions is computed using the Maximum Mean Discrepancy (MMD) criterion [42], leveraging the kernel trick to avoid dealing with the nonlinear feature space.
The MMD formulation specifies,

$$\mathrm{Dist}(p(\psi(X_S)), p(\psi(X_T))) \approx tr(W^T K M K W)) \tag{7}$$

K represents the kernel matrix, computed using a kernel function $k(x_i, x_j) = \psi(x_i)^T \psi(x_j)$. The features considered are given by X, $X = (X_S + X_T) \in \mathbb{R}^{\mathrm{NxD}}$, which is the union of the source and target features used during training, $\mathrm{N} = (\mathrm{N}_S + \mathrm{N}_T)$ is the number of training samples from the two domains, and D is their initial dimension. The Radial Basis Function (RBF) is used for the kernel,

$$k(x_i, x_j) = exp\left(\frac{||x_i - x_j||}{2l^2}\right) \tag{8}$$

In the kernel function, l is the length-scale estimated using a median heuristic [43]. The matrix $W \in \mathbb{R}^{\mathrm{Nxk}}$ is used to perform the features' transformation and reduce their dimension to k. The MMD matrix, M is defined as,

$$M(i,j) = \begin{cases} \frac{1}{\mathrm{N}_S^2}, & \text{if } x_i, x_j \in \mathcal{D}_S \\ \frac{1}{\mathrm{N}_T^2}, & \text{if } x_i, x_j \in \mathcal{D}_T \\ \frac{-1}{\mathrm{N}_S \mathrm{N}_T}, & \text{if } x_i \in \mathcal{D}_S,\ x_j \in \mathcal{D}_T \\ \frac{-1}{\mathrm{N}_T \mathrm{N}_S}, & \text{if } x_i \in \mathcal{D}_T,\ x_j \in \mathcal{D}_S \end{cases} \tag{9}$$

The TCA computes the W matrix which minimises the distance shown in Eq. (7). The MMD minimisation requires defining a centring matrix $H = I_{\mathrm{NxN}} - (1/\mathrm{N}) \cdot [1]_{\mathrm{NxN}}$, and a regularisation parameter μ. It can be written as,

$$\min_{W^T K H W = I} = tr(W^T K M K W) + \mu \cdot tr(W^T W) \tag{10}$$

Subsequently, the minimisation is written as an eigenvalue problem, employing a Lagrangian approach,

$$(K M K + \mu I) W = K H K W \psi \tag{11}$$

The resulting set of eigenvectors W, can be used to transform the features X into their latent space representation Z,

$$Z = KW \in \mathbb{R}^{\mathrm{Nxk}} \tag{12}$$

The features in the latent space can be used to compute the MSD with respect to the training features in undamaged conditions, and build a damage indicator [23]. Subsequently, any new observation is labelled according to its MSD from the samples in the undamaged conditions, comparing this distance with a threshold, which is computed via a Monte Carlo method [39] based on the dimension of the target dataset. Thus, the samples extracted from averaged FRFs in undamaged conditions can be used as training features for the source and target domains χ_S and χ_T. These features are standardised and used during training to learn a nonlinear mapping. Afterwards, the samples from the target test dataset are transformed in the latent space and their MSD is used to compute their labels. The proposed approach, comprising iFEM-based FRF reconstruction and TCA, is summarised in the flowchart of Fig. 2.

The TCA findings are compared with those obtained via a more traditional approach, as shown in [23,41,44]. This benchmark novelty-detection approach consists of using Principal Component Analysis (PCA) to learn a linear transformation of the features X_T, considered separately for each domain, to extract the essential data patterns [39]. The FRFs in X_T are transformed into a low-dimensional space. Subsequently, the same strategy based on the MSD is used to detect damage [23]. The PCA has been introduced in [45,46] for multivariate analyses. It projects a dataset into a k-dimensional space, where k is lower than the original dimension D. The new coordinates are called principal components, and they are defined to represent the largest part of the variance of the initial coordinates. Given the target features X_T, and their covariance matrix $[\Sigma_T]$, $[\Sigma_T]$ is decomposed as $[\Sigma_T] = [A][\Omega][A]^T$. The eigenvector matrix $[A] \in \mathbb{R}^{\mathrm{DxD}}$, can be truncated to $[A_r] \in \mathbb{R}^{\mathrm{Dxk}}$, which considers only the first k terms. Consequently, the principal component scores are given by $\{z\}_i = [A_r]^T(\{x_T\}_i - \{\overline{x}_T\})$ for $i = 1, ..., \mathrm{N}_T$, and $[\Omega] \in \mathbb{R}^{\mathrm{DxD}}$, is a diagonal matrix and represents the contribution of each score to the total variance of the dataset. The simplicity of PCA can be leveraged for various purposes including outlier detection, classification, variable selection, and data reduction, as presented in [47].

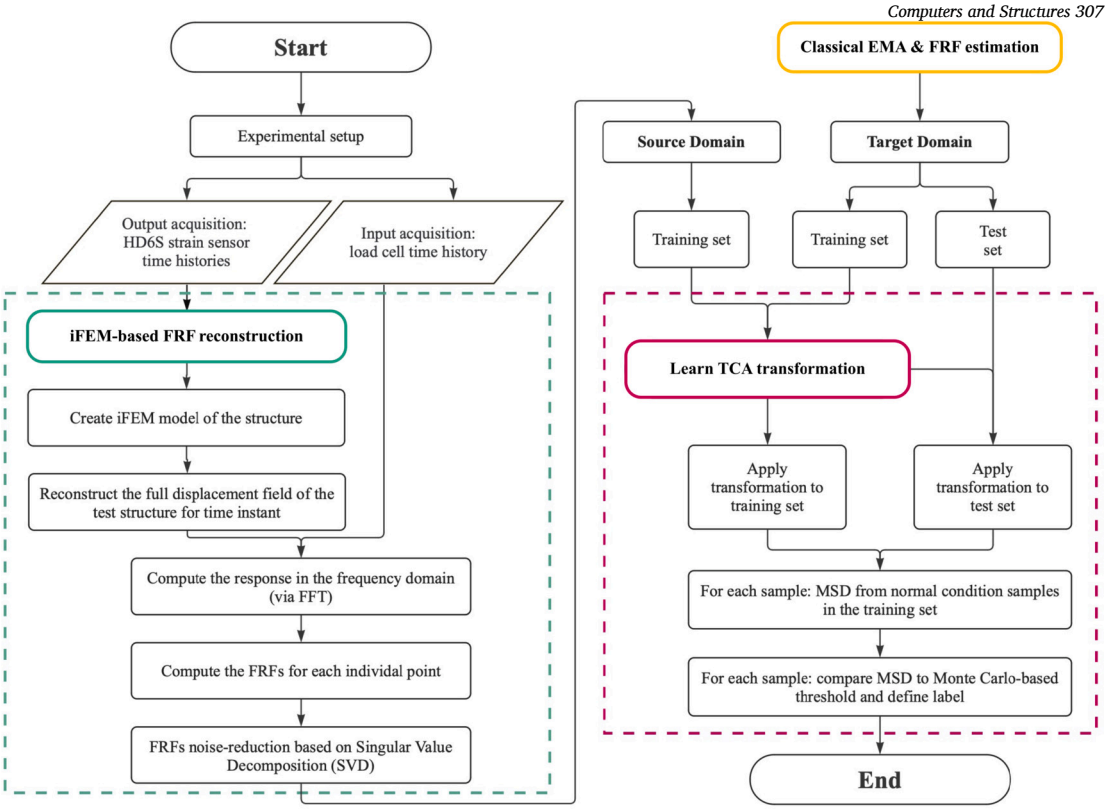

Fig. 2. Flowchart of the proposed knowledge-sharing approach, including iFEM-displacement reconstruction and FRF estimation to extract the source features.

However, this approach can be outperformed by nonlinear methods [39].

3. Experimental analysis of a population of aircraft structures

The proposed approach is analysed via two PBSHM tasks, involving a population of similar laboratory-scale aircraft, made of beam and plate components joined together via bolted connections. These structures, shown in Figs. 3 and 4, are designed according to a benchmark geometry investigated by the Structures and Materials Action Group (SM-AG19) of the Group for Aeronautical Research Technology in EURope (GARTEUR) [48]. Each structure consists of a rectangular fuselage and a rectangular plate connected to the fuselage for realising the wings. Two shorter plate elements are applied at the wingtips to simulate winglets. Finally, the model includes similar plate elements to realise the vertical and the horizontal tail. However, some sources of heterogeneity are introduced in the population by altering some materials, dimensions and geometrical details, to create a comprehensive dataset. The structures are tested with a single-input multi-output EMA approach, providing the excitation using a shaker connected to the rear of the fuselage by means of a stinger. The input is measured by a load cell at the junction between the stinger and the structure, while the responses are acquired using three different sensor setups. The tests are performed considering a baseline undamaged condition, and multiple damage conditions. The damage conditions are simulated by applying additional masses (around 2% of the aircraft mass), in multiple positions, as described in [49]. This technique induces a decrease in eigenfrequencies, which is analogous to the effect of a local stiffness loss [50,51]; thus, the discrete masses can be adopted as a reversible method for simulating damage. Indeed, the mass effect has been analysed in a finite-element model of the first steel laboratory-scale aircraft by imposing a reduction in Young's modulus of a small region on the wing, as stated in [52]. The FEM analysis found that the additional mass on the wing reduces the first natural frequency similarly to a 50% stiffness reduction of corresponding elements over 20 mm. Six damage locations are considered in the classical EMA tests: one at the wing tip, two along the wing, one on the horizontal tail and two on the fuselage, at the tip and the end. Instead, the strain-based EMA has been performed considering only the third mass location on the wing, and the damage location on the horizontal tail.

The first PBSHM case study involves two laboratory-scale steel aircraft, shown in Fig. 3. The first one (Fig. 3a) has a 2.0 m wingspan, and its fuselage is built using a thin-section Fe360 profile, with a length of 1.5 m and a thickness of 3.0 mm. The wings and the other elements are built using S235JRC+C steel plate elements, 8.0 mm thick and 100.0 mm wide. This structure is tested twice, adopting a periodic chirp excitation and acquiring the response via high-definition distributed fibre-optic strain sensors and SLDV, producing two dissimilar datasets from the same system. The second structure (Fig. 3b) is almost identical to the first one. The only differences regard the fuselage profile - which is solid - and manufacturing variations in the plates' thickness. This aircraft is tested by adopting ICP accelerometers, producing a third dataset. Subsequently, these three datasets are used to perform knowledge transfer in a homogeneous framework, because the systems are almost identical. In particular, iFEM is used to harmonise the features extracted from the strain-based EMA, as presented in [21], and the resulting features are used as a source domain for enhancing damage detection on the other two datasets, solving the issue of different experimental setups.

The second PBSHM case study includes a different aircraft model (Fig. 4), which differs from the first one in terms of materials, scaling and winglet configuration. To ensure clear and consistent identification, the name of each model is defined by its size, material, and a numerical identifier to differentiate models of the same material and scale. This convention supports a systematic expansion of the aircraft population, as developed in [53]. This structure is made of aluminium, it has a wingspan of 1.0 m and it does not have winglets. Instead, this structure includes some additional elements connected to the wings to simulate the engine's weight. Additionally, this aircraft is tested by adopting the SLDV in a classical EMA setup. This task adopts the iFEM-reconstructed features as a source domain, and the SLDV features from the aluminium aircraft as a target domain. Each test provides the FRF at

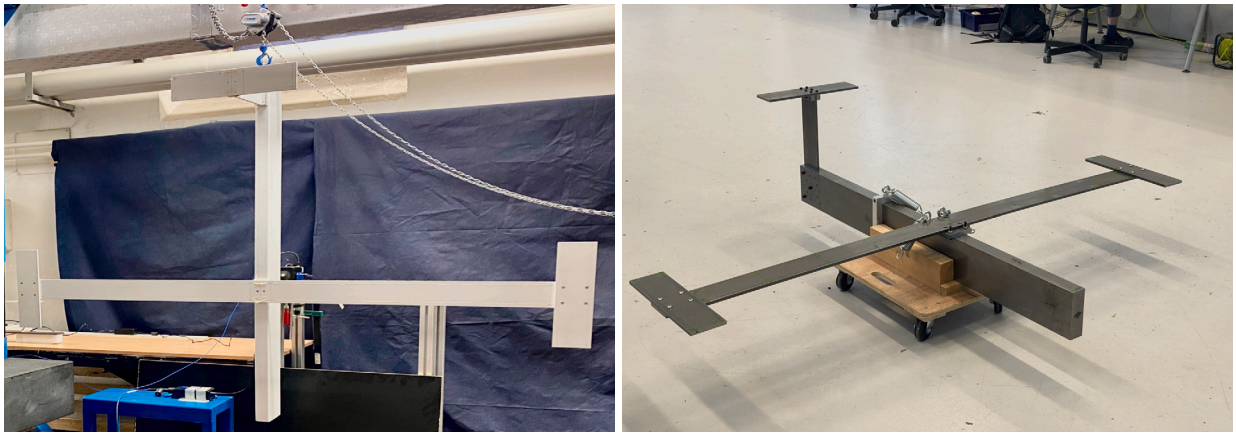

(a) Large steel aircraft with end winglets (#1).

(b) Large steel aircraft with end winglets (#2).

Fig. 3. Pictures of the aircraft structures for the homogeneous case study.

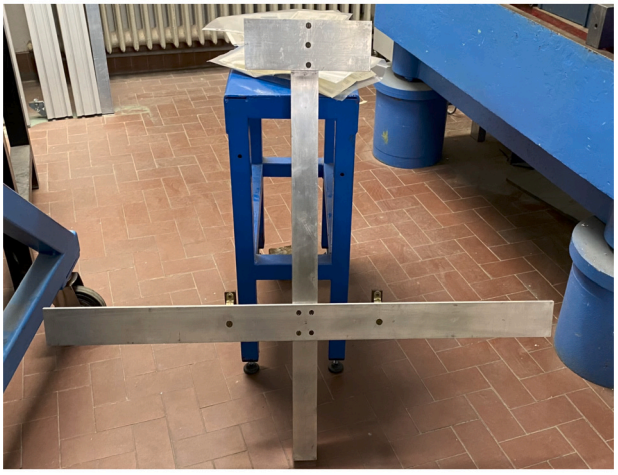

Fig. 4. Picture of the small aluminium aircraft (#1) for the heterogeneous case study.

all the measurement points and the summed FRF. The features are computed from the normalised amplitude of the summed FRFs to consider global quantities. The iFEM-reconstructed transfer function is shown in Fig. 5, and the corresponding dataset is computed from the measurements by polluting the normalised FRFs with $\sigma = 0.1$ Gaussian noise relative to the normalised amplitude. The tests have been carried out in the "LAQ-AERMEC Aeromechanical Structural Systems" laboratory of the Department of Mechanical and Aerospace Engineering, Politecnico di Torino, and the "Laboratory for Verification and Validation " (LVV), The University of Sheffield.

These functions are extracted from the strain time histories measured by the high-definition distributed fibre-optic sensors. Specifically, iFEM is adopted to reconstruct the displacement time histories at each measurement point, the response is evaluated in the frequency domain via FFT, and the FRF is computed by means of the H1 estimator, exploiting the load-cell input measurements. Further details on the experimental campaign and the strain-based features before and after iFEM-based displacement reconstruction can be found in [21]. Analogously, it is possible to create the dataset and extract the displacement FRFs measured in the classical EMA tests. These features are shown in Fig. 6. The FRFs shown in Figs. 5 and 6 are computed over 2048 spectral lines, and the analysed frequency range depends on the specific case study. Specifically, a 0-50 Hz range is analysed for the large steel aircraft, to represent the first main flexural vibration modes and the first torsional modes of the wings. Instead, a wider range (0-320 Hz) is analysed for the small aluminium model to analyse corresponding vibration modes. The extracted features consist of FRF segments, being equivalent in terms of the number of spectral lines, evaluated around the peaks of the main vibration modes identified in the measured frequency range. Thus, only the most significant parts of the FRFs are considered and the dimensionality of the extracted features is reduced from 2048 to 861.

4. Results

The current section describes the damage detection results obtained using TCA on the three analysed target domains, sharing the knowledge acquired from the iFEM-reconstructed features of the large steel aircraft (#1). The first two pairs of source and target domains represent analogous structures, to focus on harmonising different sensor setups; the third transfer learning case study considers two dissimilar source and target structures, to extend the application of iFEM-reconstructed features for heterogeneous problems. Additionally, the transfer-learning results are compared to the benchmark novelty-detection approach based on PCA and MSD to highlight how knowledge transfer and the PBSHM approach can improve damage identification.

4.1. Baseline damage detection on the individual datasets

The PCA is applied to the individual FRFs of each target for understanding the achievable performance in the absence of knowledge transfer. A dataset is produced for each domain by splitting its features into a training and a test set. Assuming that only a few experimental data can be measured in the potential target, the training set only includes five samples from the undamaged condition, and the test set comprises five samples from the undamaged condition and one sample for each damaged condition. The PCA produces a feature transformation into a k-dimensional space, with $k = 2$ to aid visualisation. This transformation is applied to the test data, and the MSD from the samples in the undamaged conditions provides the damage indicator. The MSD between the PCA-transformed samples is shown in Fig. 7. The results can be presented in terms of the undamaged condition samples, True Negative Rates (TNR), and True Positive Rates (TPR), i.e., correctly labelled samples from the damaged conditions. These results are presented in Fig. 7d, showing how, although the undamaged condition samples are correctly identified, the TPRs are significantly lower. Fig. 7d shows the averaged performance over 100 repetitions, computed to reduce the influence of the sampling process on the findings.

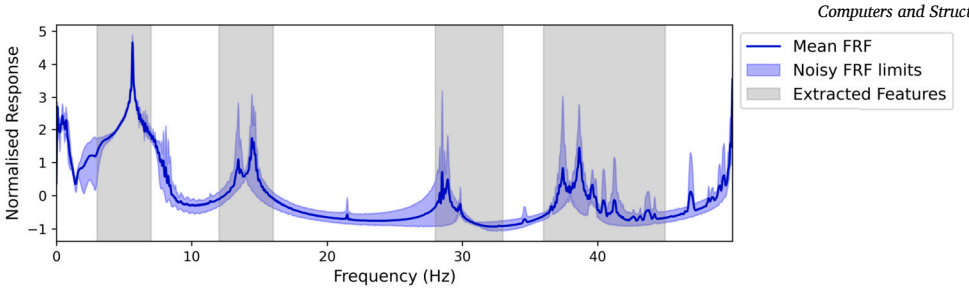

Fig. 5. Normalised noisy displacement FRF, extracted from the strain measurements via iFEM-displacement reconstruction on the large steel aircraft with end winglets (#1). The extracted features are shown in shaded grey.

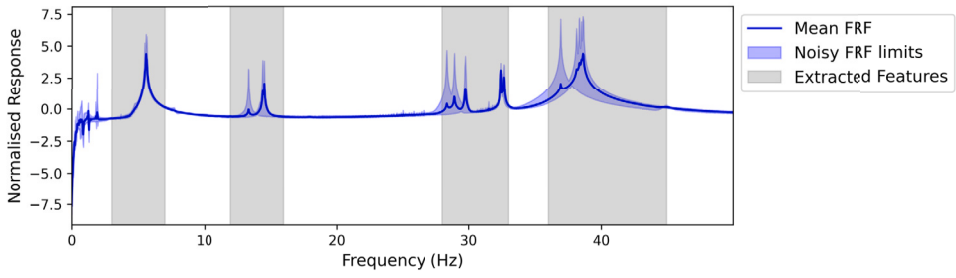

(a) Large steel aircraft with end winglets (#1).

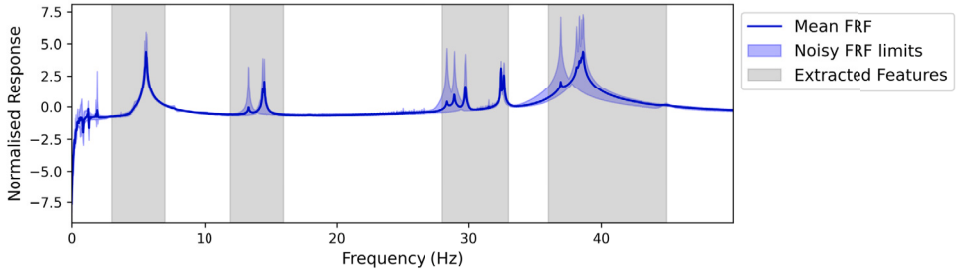

(b) Large steel aircraft with end winglets (#2).

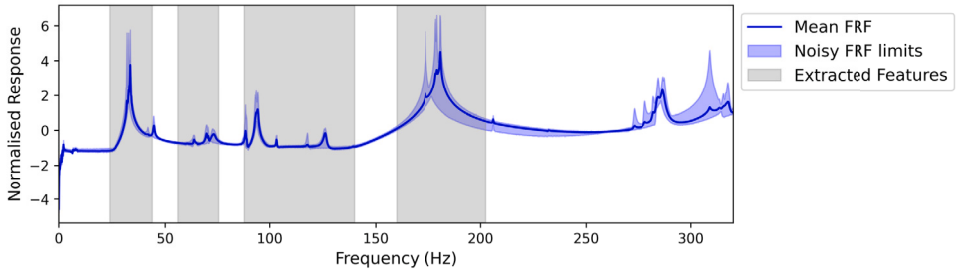

(c) Small aluminium aircraft with no winglets (#1).

Fig. 6. Normalised noisy displacement FRFs of the target domains, computed by polluting the measurements with Gaussian noise, and extracted features in shaded grey.

4.2. Knowledge sharing between analogous structures and different sensor setups

The current section includes the first two knowledge-sharing tasks, in which the iFEM-reconstructed features (Fig. 5) are exploited as the source dataset to improve damage detection performance on two analogous structures (Figs. 6a and 6b). The target domain refers to the dataset presented for the baseline comparison. Instead, the source dataset is extracted analogously from the displacement FRFs, but that is assumed to be twice as large as the target dataset. Therefore, only samples collected from undamaged conditions are employed during the training process. The number of components k in the TCA is defined as equal to the number of components evaluated in the PCA to aid comparison. The TCA is adopted to map the normalised features in a common latent space, as shown in Fig. 8a for the first target structure and Fig. 9a for the second target structure. The new samples are labelled according to the MSD between the test samples and the transformed training features in the undamaged condition. The MSD results are shown in Fig. 8b for the first target structure and Fig. 9b for the second target structure.

The results of this task, which focussed on a homogeneous case study, show that including the iFEM-reconstructed source data in the proposed transfer-learning strategy can create a valuable latent representation of features. This representation enables the source and target samples from normal conditions to form a single cluster. In contrast, the samples from

(a) Large steel aircraft (#1) SLDV features.

(b) Large steel aircraft (#2) Accelerometers features.

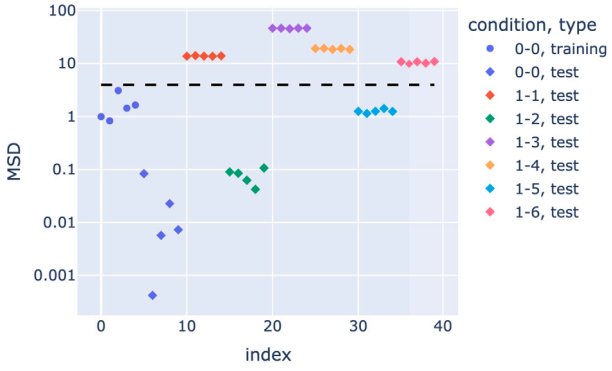

(c) Small aluminium aircraft (#1) SLDV features.

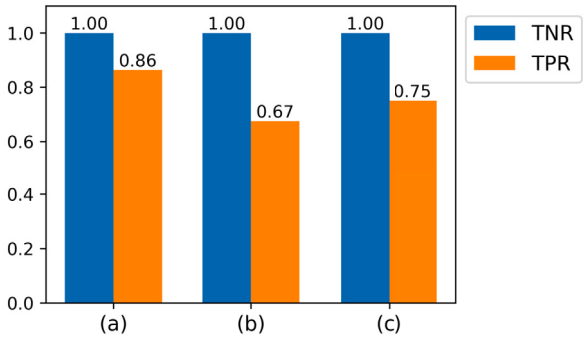

(d) Results summary: TNRs and TPRs.

Fig. 7. Results of the benchmark PCA and MSD analysis applied on the individual datasets. The label "0-0" refers to the undamaged condition, and the label "1-n" refers to a damaged condition, where n defines the damage location.

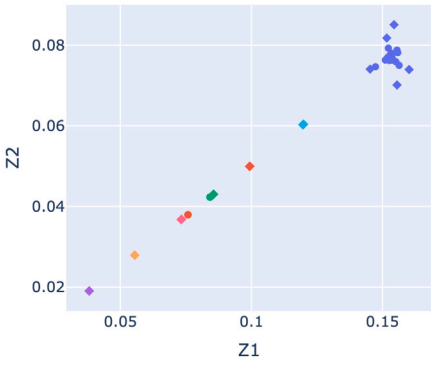

(a) Transformed features in the latent space.

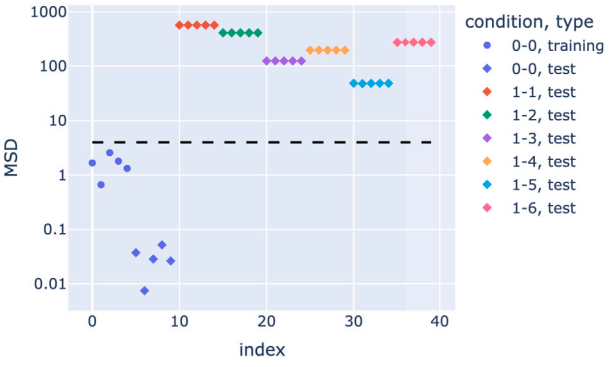

(b) MSD results.

Fig. 8. Results of the TCA and MSD analysis applied using the iFEM-reconstructed features as the source domain and the SLDV FRFs acquired from the large steel aircraft (#1).

damaged conditions deviate significantly from this cluster, facilitating their identification. As a result, the MSD of these samples is much higher than the defined threshold, leading to improved outlier detection performance.

4.3. Knowledge sharing between heterogeneous structures and different sensor setups

The third knowledge-sharing task exploits the previously-seen iFEM-reconstructed dataset as the source domain to improve damage-detection performance on a dissimilar structure, i.e., the small aluminium aircraft (Fig. 6c). The target data refer to the dataset already presented for the baseline comparison. The source and target features are transformed to a common latent space by means of TCA, as shown in 10a. Subsequently, the transformed samples from the test dataset of the target domain are labelled according to the MSD from the transformed training features in the undamaged condition. The MSD results are shown in Fig. 10b.

Similarly to the previous case study, the knowledge-sharing process outperforms the baseline damage detection. In this case, not only the sensor setups but also the geometrical and material properties of the target structure differ from those of the source. Regardless, the iFEM-reconstructed features are accurately harmonised with the segments of displacement FRFs acquired from the small aluminium aircraft model. Consequently, the samples from undamaged conditions are mapped in

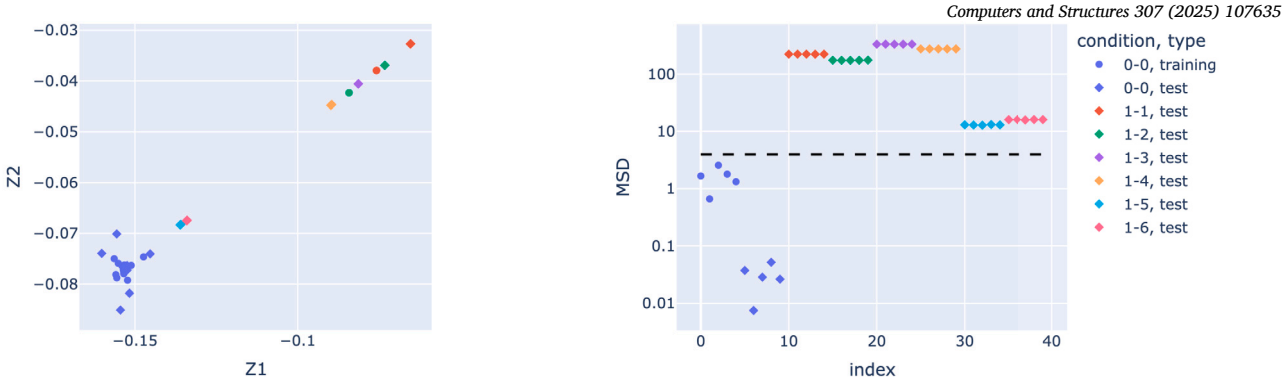

(a) Transformed features in the latent space. (b) MSD results.

Fig. 9. Results of the TCA and MSD analysis applied using the iFEM-reconstructed features from the large steel aircraft (#1) as the source domain and the FRFs acquired from the large steel aircraft (#2).

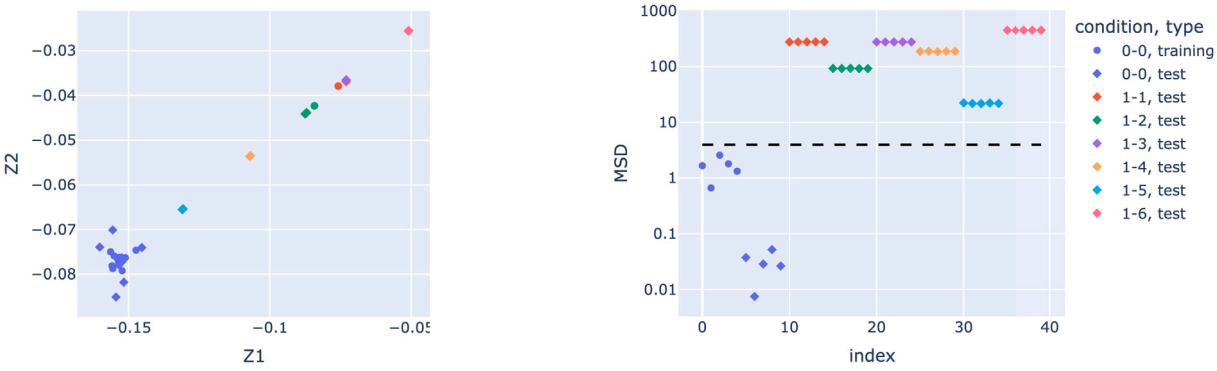

(a) Transformed features in the latent space. (b) MSD results.

Fig. 10. Results of the TCA and MSD analysis applied using the iFEM-reconstructed features from the large steel aircraft (#1) as the source domain and the FRFs acquired from the small aluminium aircraft (#1).

Table 1
Results summary for the knowledge-transfer tasks: TNRs, TPRs and F1 score.

Source	Target	TNR	TPR	F1 score
Large steel a. (#1)- iFEM	Large steel a. (#1) - SLDV	1.00	0.98	0.99
Large steel a. (#1)- iFEM	Large steel a. (#2) - Accels.	1.00	0.92	0.95
Large steel a. (#1)- iFEM	Small aluminium a. (#1) - SLDV	1.00	0.94	0.97

a single cluster, and the MSD of the samples acquired from damaged conditions are higher than the identification threshold.

The overall performance of the two case studies can be analysed in terms of TNRs, TPRs and F1 score, which measures the accuracy of the test. These results, shown in Table 1, regard the averaged performance over 100 repetitions, computed to reduce the influence of the sampling process on the findings. The three transfer-learning tasks correctly identify all the samples in the undamaged conditions. Additionally, TCA significantly improves the detection of samples from damaged conditions (TPRs) with respect to the baseline approach (Fig. 7d), leading to high accuracy, as shown by the F1 scores.

5. Discussions and conclusions

This study proposes including the iFEM shape-sensing method in the PBSHM approach to facilitate data-driven damage detection. Indeed, PBSHM exploits transfer-learning algorithms to leverage knowledge from similar structures in a population and perform efficient SHM. In this framework, iFEM is exploited preliminarily for reconstructing the dynamic features from a strain-based EMA, harmonising the experimental findings to the classical features adopted in vibration-based SHM. The iFEM capability of extracting displacement FRFs and modal properties from dynamic strain measurements has already been presented in the first part of this study [21]. Accordingly, the current work focusses on the knowledge-sharing process, exploiting iFEM-reconstructed features as a source domain.

This approach is implemented on an experimental population of similar laboratory-scale aircraft, measuring their dynamic response with three different sensor setups and simulating different damaged conditions. The iFEM-reconstructed FRFs from the first large steel aircraft model are used to extract damage-sensitive features and build a source domain. These features are transferred to a different target domain employing the TCA algorithm. TCA maps the features into a common space, where damage detection is performed by computing the MSD to the cluster of undamaged condition samples. The knowledge-sharing process is investigated via two different tasks. First, it is applied to almost identical structures (with manufacturing variations only). Subsequently, the same strategy is applied to a new target structure, a small aluminium aircraft model with no winglets, exploiting the same iFEM-reconstructed source dataset. In addition, the approach based on iFEM and PBSHM is compared to a baseline damage-detection strategy based on PCA. The overall findings illustrate that the proposed approach can improve damage de-

tection compared to the baseline strategy, as shown by the performance indicators in Table 1. Specifically, the first two tasks study the problem of knowledge transfer within a homogeneous population, tested via three different types of instrumentation (high-definition distributed fibre-optic strain sensors, SLDV and ICP accelerometers), showing that iFEM can be used to deal with results obtained from varying experimental setups, sensors, inputs, and acquisition systems. The third task extends this approach to a more heterogeneous knowledge-sharing problem, including multiple differences between the source and the target structures (i.e., topological, material and geometrical properties). The significant improvement in the damage-detection performance obtained in this case shows that the features extracted from dynamic strain measurements employing iFEM can provide reliable datasets.

Embedding iFEM in this strategy enhances estimating the global dynamic response and modal parameters of an analysed structure from a cost-effective sensor scheme, producing a comprehensive dataset of damage-sensitive features without a priori knowledge of the critical locations. In contrast, traditional techniques often require a greater number of sensors or may only capture the FRF at a single location. These configurations may result in insufficient data for analysing the overall dynamic behaviour of the structure, limiting the approach to a more localised perspective. Moreover, this methodology can be efficiently integrated into PBSHM, providing real-time features for monitoring fleets or populations of similar structures via similarity assessment and domain-adaptation algorithms. While the current work focusses on the challenges related to knowledge transfer, both the two PBSHM phases are crucial to deal with heterogeneous structures, and iFEM can provide added value in both. The ability of iFEM to reconstruct full-field mode shape data across the structure allows for a richer dataset that can enhance similarity assessment, providing a physics-based approach to measure the similarity within the population and reducing the risk of negative transfer. Subsequently, the harmonised damage-sensitive features can provide reliable source information to inform new monitoring tasks, as shown by the experimental results. Therefore, the proposed strategy extends PBSHM feasibility in real-world applications by managing heterogeneous data types produced by different experimental setups, sensors, inputs, and acquisition systems in the knowledge-sharing process and enhancing damage detection performance. Further developments may concern using these comprehensive and detailed features in the similarity assessment process and more complicated tasks such as damage localisation and quantification across heterogeneous populations of structures.

CRediT authorship contribution statement

Giulia Delo: Writing – review & editing, Writing – original draft, Software, Methodology, Investigation, Data curation, Conceptualization. **Rinto Roy:** Writing – original draft, Software, Methodology, Investigation, Data curation, Conceptualization. **Keith Worden:** Writing – review & editing, Supervision, Methodology, Investigation, Funding acquisition, Conceptualization. **Cecilia Surace:** Writing – review & editing, Supervision, Methodology, Investigation, Funding acquisition, Conceptualization.

Declaration of competing interest

The authors declare the following financial interests/personal relationships which may be considered as potential competing interests: Keith Worden reports financial support was provided by Engineering and Physical Sciences Research Council. If there are other authors, they declare that they have no known competing financial interests or personal relationships that could have appeared to influence the work reported in this paper.

Acknowledgement

The authors of this paper gratefully acknowledge the support of the UK Engineering and Physical Sciences Research Council (EPSRC) via grant reference EP/W005816/1. For the purpose of open access, the authors have applied a Creative Commons Attribution (CC BY) licence to any Author Accepted Manuscript version arising.

Data availability

Data will be made available on request.

References

[1] Cawley P. Structural health monitoring: closing the gap between research and industrial deployment. Struct Health Monit 2018;17(5):1225–44. https://doi.org/10.1177/1475921717750047.
[2] Gherlone M, Mattone M, Surace C, Tassotti A, Tessler A. Novel vibration-based methods for detecting delamination damage in composite plate and shell laminates. Key Eng Mater 2005;293:289–96.
[3] Gherlone M, Cerracchio P, Mattone M. Shape sensing methods: review and experimental comparison on a wing-shaped plate. Prog Aerosp Sci 2018;99:14–26. https://doi.org/10.1016/j.paerosci.2018.04.001.
[4] Roy R. Developing advanced shape sensing methodologies for aerospace applications. Ph.D. thesis. Politecnico di Torino; 2022.
[5] Vazquez SL, Tessler A, Quach CC, Cooper EG, Parks J, Spangler JL. Structural health monitoring using high-density fiber optic strain sensor and inverse finite element methods. Tech rep; 2005.
[6] Dong C-Z, Catbas FN. A review of computer vision–based structural health monitoring at local and global levels. Struct Health Monit 2021;20(2):692–743.
[7] Tessler A. Structural analysis methods for structural health management of future aerospace vehicles. Key Eng Mater 2007;347:57–66.
[8] Tessler A, Riggs HR, Freese CE, Cook GM. An improved variational method for finite element stress recovery and a posteriori error estimation. Comput Methods Appl Mech Eng 1998;155(1–2):15–30.
[9] Tessler A. A variational principle for reconstruction of elastic deformations in shear deformable plates and shells, national aeronautics and space administration. Langley Research Center; 2003.
[10] Tessler A, Spangler JL. A least-squares variational method for full-field reconstruction of elastic deformations in shear-deformable plates and shells. Comput Methods Appl Mech Eng 2005;194(2–5):327–39.
[11] Cerracchio P, Gherlone M, Mattone MC, Di Sciuva M, Tessler A, et al. Shape sensing of three-dimensional frame structures using the inverse finite element method. In: Proceedings of the V European workshop on structural health monitoring. DESTech Publications Inc.; 2010. p. 615–20.
[12] Gherlone M, Cerracchio P, Mattone M, Di Sciuva M, Tessler A. Shape sensing of 3d frame structures using an inverse finite element method. Int J Solids Struct 2012;49(22):3100–12.
[13] Roy R, Gherlone M, Surace C. A shape sensing methodology for beams with generic cross-sections: application to airfoil beams. Aerosp Sci Technol 2021;110:106484. https://doi.org/10.1016/j.ast.2020.106484.
[14] Roy R, Surace C, Gherlone M. Full-field deformation reconstruction of beams using the inverse finite element method: application to thin-walled structures. Thin-Walled Struct 2024;200:111907. https://doi.org/10.1016/j.tws.2024.111907. https://www.sciencedirect.com/science/article/pii/S0263823124003501.
[15] Gherlone M, Cerracchio P, Mattone M, Sciuva MD, Tessler A. An inverse finite element method for beam shape sensing: theoretical framework and experimental validation. Smart Mater Struct 2014;23(4):045027. https://doi.org/10.1088/0964-1726/23/4/045027.
[16] Roy R, Tessler A, Surace C, Gherlone M. Efficient shape sensing of plate structures using the inverse finite element method aided by strain pre-extrapolation. Thin-Walled Struct 2022;180:109798. https://doi.org/10.1016/j.tws.2022.109798.
[17] Li M, Kefal A, Oterkus E, Oterkus S. Structural health monitoring of an offshore wind turbine tower using ifem methodology. Ocean Eng 2020;204:107291. https://doi.org/10.1016/j.oceaneng.2020.107291. https://www.sciencedirect.com/science/article/pii/S0029801820303346.
[18] Li M, Jia D, Wu Z, Qiu S, He W. Structural damage identification using strain mode differences by the ifem based on the convolutional neural network (cnn). Mech Syst Signal Process 2022;165:108289. https://doi.org/10.1016/j.ymssp.2021.108289.
[19] Oboe D, Poloni D, Sbarufatti C, Giglio M. Towards automatic crack size estimation with ifem for structural health monitoring. Sensors 2023;23(7). https://doi.org/10.3390/s23073406.
[20] Esposito M. A novel shape sensing approach based on the coupling of modal virtual sensor expansion and ifem: numerical and experimental assessment on composite stiffened structures. Comput Struct 2024;305:107520.
[21] Delo G, Roy R, Worden K, Surace C. Using the inverse finite-element method to harmonise classical modal analysis with fibre-optic strain data for robust population-based structural health monitoring. Strain 2024;e12481. https://doi.org/10.1111/str.12481.

[22] Belur MY, Kefal A, Abdollahzadeh MA, Fassois SD. Damage diagnosis of plates and shells through modal parameters reconstruction using inverse finite-element method. Struct Health Monit 2024. https://doi.org/10.1177/14759217241249678.
[23] Worden K, Manson G, Fieller NR. Damage detection using outlier analysis. J Sound Vib 2000;229(3):647–67.
[24] Worden K, Manson G. The application of machine learning to structural health monitoring. Philos Trans - Royal Soc, Math Phys Eng Sci 2007;365(1851):515–37.
[25] Rytter A. Vibrational based inspection of civil engineering structures. 1993.
[26] Gardner P, Liu X, Worden K. On the application of domain adaptation in structural health monitoring. Mech Syst Signal Process 2020;138:106550.
[27] Bull LA, Gardner PA, Gosliga J, Rogers TJ, Dervilis N, Cross EJ, et al. Foundations of population-based SHM, part I: homogeneous populations and forms. Mech Syst Signal Process 2021;148:107141.
[28] Gosliga J, Gardner PA, Bull LA, Dervilis N, Worden K. Foundations of population-based SHM, part II: heterogeneous populations–graphs, networks, and communities. Mech Syst Signal Process 2021;148:107144.
[29] Gardner PA, Bull LA, Gosliga J, Dervilis N, Worden K. Foundations of population-based SHM, part III: heterogeneous populations–mapping and transfer. Mech Syst Signal Process 2021;149:107142.
[30] Tsialiamanis G, Mylonas C, Chatzi E, Dervilis N, Wagg DJ, Worden K. Foundations of population-based shm, part iv: the geometry of spaces of structures and their feature spaces. Mech Syst Signal Process 2021;157:107692.
[31] Delo G, Bunce A, Cross E, Gosliga J, Hester D, Surace C, et al. When is a bridge not an aeroplane? Part II: a population of real structures. In: European workshop on structural health monitoring: EWSHM 2022-volume 2. Springer; 2022. p. 965–74.
[32] Delo G, Surace C, Worden K, Brennan DS. On the influence of structural attributes for assessing similarity in population-based structural health monitoring. In: Proceedings of the 14th international workshop on structural health monitoring 2023: designing SHM for sustainability, maintainability, and reliability. DEStech Publications, Inc.; 2023.
[33] Rosenstein MT, Marx Z, Kaelbling LP, Dietterich TG. To transfer or not to transfer. In: NIPS 2005 workshop on transfer learning, vol. 898; 2005.
[34] Hughes AJ, Delo G, Poole J, Dervilis N, Worden K. Quantifying the value of positive transfer: an experimental case study. In: Proceedings of the 11th European workshop on structural health monitoring (EWSHM2024); 2024.
[35] Delo G, Hughes AJ, Surace C, Worden K. On the influence of attributes for assessing similarity and sharing knowledge in heterogeneous populations of structures. Available at SSRN. https://doi.org/10.2139/ssrn.5006357, 2024.
[36] Hughes AJ, Poole J, Dervilis N, Gardner P, Worden K. A decision framework for selecting information-transfer strategies in population-based shm. arXiv:2307.06978. https://arxiv.org/abs/2307.06978, 2023.
[37] Pan SJ, Yang Q. A survey on transfer learning. IEEE Trans Knowl Data Eng 2009;22(10):1345–59.
[38] Pan SJ, Tsang IW, Kwok JT, Yang Q. Domain adaptation via transfer component analysis. IEEE Trans Neural Netw 2010;22(2):199–210.
[39] Farrar CR, Worden K. Structural health monitoring: a machine learning perspective. John Wiley & Sons; 2012.
[40] Yang Q, Zhang Y, Dai W, Pan SJ. Transfer learning. Cambridge University Press; 2020.
[41] Bull L, Gardner P, Dervilis N, Papatheou E, Haywood-Alexander M, Mills R, et al. On the transfer of damage detectors between structures: an experimental case study. J Sound Vib 2021;501:116072.
[42] Gretton A, Borgwardt KM, Rasch MJ, Schölkopf B, Smola A. A kernel method for the two-sample-problem. Adv Neural Inf Process Syst 2006;19.
[43] Gretton A, Borgwardt KM, Rasch MJ, Schölkopf B, Smola A. A kernel two-sample test. J Mach Learn Res 2012;13(1):723–73.
[44] Delo G, Brennan DS, Surace C, Worden K. On the influence of structural attributes for transferring knowledge in population-based structural health monitoring. In: Proceedings of the 42nd international conference on modal analysis (IMAC-XLII); 2024.
[45] Pearson K. Liii. on lines and planes of closest fit to systems of points in space. Lond Edinb Dublin Philos Mag J Sci 1901;2(11):559–72.
[46] Hotelling H. Analysis of a complex of statistical variables into principal components. J Educ Psychol 1933;24(6):417.
[47] Wold S, Esbensen K, Geladi P. Principal component analysis. Chemom Intell Lab Syst 1987;2(1–3):37–52.
[48] Link M, Friswell M. Working group 1: generation of validated structural dynamic models - results of a benchmark study utilising the garteur sm-ag19 test-bed. Mech Syst Signal Process 2003;17(1):9–20. https://doi.org/10.1006/mssp.2002.1534.
[49] Delo G, Mattone M, Surace C, Worden K. Novelty detection across a small population of real structures: a negative-selection approach. In: XII international conference on structural dynamics; 2023.
[50] Papatheou E, Manson G, Barthorpe RJ, Worden K. The use of pseudo-faults for novelty detection in SHM. J Sound Vib 2010;329(12):2349–66. https://doi.org/10.1016/j.jsv.2009.07.020.
[51] Behmanesh I, Moaveni B. Probabilistic identification of simulated damage on the dowling Hall footbridge through Bayesian finite element model updating. Struct Control Health Monit 2015;22(3):463–83.
[52] Friswell M, Penny J, Garvey S. A combined genetic and eigensensitivity algorithm for the location of damage in structures. Comput Struct 1998;69(5):547–56. https://doi.org/10.1016/S0045-7949(98)00125-4.
[53] Delo G, Surace C, Worden K. Knowledge sharing for improving damage identification across a population of heterogeneous laboratory-scale aircraft models. In: Proceedings of the 31st international conference on noise and vibration engineering (ISMA 2022). KU Leuven Department of Mechanical Engineering; 2024.